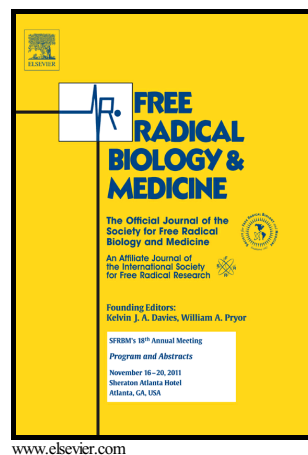


Author's Accepted Manuscript

UV cell stress induces oxidative cyclization of a protective reagent for DNA damage reduction in skin explants

Jing Liu, Haizhou Zhu, Gurdat Premnauth, Kaylin G. Earnest, Patricia Hahn, George Gray, Jack A. Queenan, Lisa E. Prevette, Safnas F. AbdulSalam, Ana Luisa Kadekaro, Edward J. Merino



PII: S0891-5849(18)31268-1
DOI: <https://doi.org/10.1016/j.freeradbiomed.2018.12.037>
Reference: FRB14097

To appear in: *Free Radical Biology and Medicine*

Received date: 23 July 2018
Revised date: 10 December 2018
Accepted date: 29 December 2018

Cite this article as: Jing Liu, Haizhou Zhu, Gurdat Premnauth, Kaylin G. Earnest, Patricia Hahn, George Gray, Jack A. Queenan, Lisa E. Prevette, Safnas F. AbdulSalam, Ana Luisa Kadekaro and Edward J. Merino, UV cell stress induces oxidative cyclization of a protective reagent for DNA damage reduction in skin explants, *Free Radical Biology and Medicine*, <https://doi.org/10.1016/j.freeradbiomed.2018.12.037>

This is a PDF file of an unedited manuscript that has been accepted for publication. As a service to our customers we are providing this early version of the manuscript. The manuscript will undergo copyediting, typesetting, and review of the resulting galley proof before it is published in its final citable form. Please note that during the production process errors may be discovered which could affect the content, and all legal disclaimers that apply to the journal pertain.

UV cell stress induces oxidative cyclization of a protective reagent for DNA damage reduction in skin explants

Jing Liu^a, Haizhou Zhu^a, Gurdat Premnauth, Kaylin G Earnest^a, Patricia Hahn^a, George Gray^a, Jack A. Queenan^b, Lisa E. Prevette^b, Safnas F AbdulSalam^a, Ana Luisa Kadekaro^c, Edward J Merino^{a,*}

^aDepartment of Chemistry, McMicken College of Arts and Sciences, University of Cincinnati, Cincinnati, OH, USA

^bDepartment of Chemistry, University of St. Thomas, St. Paul, MN, USA

^cDepartment of Dermatology, College of Medicine, University of Cincinnati, Cincinnati, OH, USA

*Corresponding author: *Email address:* merinoed@ucmail.uc.edu (Edward J Merino)

Abstract:

UV irradiation is a major driver of DNA damage and ultimately skin cancer. UV exposure leads to persistent radicals that generate ROS over prolonged periods of time. Toward the goal of developing long-lasting antioxidants that can penetrate skin, we have designed a ROS-initiated protective (RIP) reagent that, upon reaction with ROS (antioxidant activity), self-cyclizes and then releases the natural product apocynin. Apocynin is a known antioxidant and inhibitor of NOX oxidase enzymes. A key phenol on the compound **1** controls ROS-initiated cyclization and makes **1** responsive to ROS with a EC₅₀ comparable to common antioxidants in an ABTS assay. In an *in vitro* DNA nicking assay, the RIP reagent prevented DNA strand breaks. In cell-based assays, the reagent was not cytotoxic, apocynin was released only in cells treated with UVR, reduced UVR-induced cell death, and lowered DNA lesion formation. Finally, topical treatment of human skin explants with the RIP reagent reduced UV-induced DNA damage as monitored by quantification of cyclobutane dimer formation and DNA repair signaling via TP53. The reagent was more effective than administration of a catalase antioxidant on skin explants. This chemistry platform will expand the types of ROS-activated motifs and enable inhibitor release for potential use as a long-acting sunscreen.

Graphical Abstract



Keywords: ROS, antioxidant, apocynin, reactive oxygen species, melanoma, UV, sunscreen, radical

1. Introduction

Prolonged exposure to ultraviolet radiation (UVR) generates reactive oxygen species (ROS) forms that are highly toxic. [1] UVR-mediated excitation of melanin and ROS imbalance are important biochemical contributors to melanoma risk. [2] Counterintuitively, skin cells, especially melanocytes, have benign biochemistry that generates and utilizes ROS (Figure 1) such as hydrogen

peroxide. These normal biochemical functions include melanin production and protein signaling. [3] Recently, it has been found that UVR not only causes direct DNA damaging events but also results in the generation of “dark” cyclobutane pyrimidine dimers (CPDs), which derive from radicals long after exposure. [4] Melanin-based radicals, observed using electron paramagnetic resonance experiments, can generate the more toxic hydroxyl radical (Figure 1) long after UVR exposure. These radicals lead to the production of exotic DNA damage products that are both lethal and mutagenic. [5] Currently available sunscreens, which are comprised of UVR blocking and UVR absorbing compounds, combat excessive UV exposure but do not stop these dark damaging events. In addition, marine life toxicity issues surrounding the use of UVR-blocking compounds like oxybenzone and the finding that repetitive sunburns are strongly associated with poor prognosis melanoma mean that new sun-protection agents are needed. There are two design requirements: (I) minimal activity against benign ROS biochemistry and (II) a non-stoichiometric or catalytic cellular effect to enhance activity. In this manuscript, we detail our first molecular design that satisfies these criteria. The ROS-initiated protective (RIP) reagent reported here releases the natural product apocynin, an inhibitor of NADPH oxidases, upon oxidative reactions with ROS generated in cells by UVR and later forming “dark” damage events (Figure 1).

We were among the first to report ROS-activated chemotherapeutic agents. [6, 7] The most common ROS-responsive chemistries are boron-based. Boron-based antioxidants, [8, 9] modified gene-targeting agents, [10] and inhibitor pro-drugs have been reported. [11, 12] Alternatives are needed for several reasons. First, aryl boronate esters readily oxidize in the presence of hydrogen peroxide or other ROS forms in a Chan-lam-like reaction. [13] Given that the steady-state concentration of peroxide in blood and cells is between 200 nM and 2 μ M, [14] reported aryl boronate esters are likely activated rapidly *in vivo*. We have used a much different approach in this

work that spans several molecular designs. [15] We designed a cytotoxic molecule a few years back. [16] This molecule had an unusual mechanism in that it underwent intramolecular cyclization and dehydrated in the presence of hydrogen peroxide. Then we designed an antioxidant that was not cytotoxic but this molecule had modest cell effects. [17, 18] In this work we hypothesized that biologically-relevant effects could be achieved by taking advantage of this oxidative reaction pathway to eject a bioactive inhibitor of ROS-producing enzymes for UVR induced protection (**1**, Figure 1). We reasoned if we could release an inhibitor of cellular oxidases, like apocynin (red, Figure 1), then selectively initiated cellular protection would be possible. This manuscript details our first investigations into addition of a bioactive molecule to generate catalytic antioxidants.

We sought to design a RIP reagent that would activate and release a bioactive molecule that could globally lower ROS selectively (SI Scheme 1 for mechanism). This is important because unselective ROS reduction can be harmful. [19] A survey of literature identified several NADPH oxidase inhibitors that act as general ROS reducers. We focused on a natural product called apocynin (Figure 1), a ketone version of vanilla, that has been used in traditional medicines. Its promiscuous biological properties are ascribed to the ability to inhibit oxidases in the monomeric and multimeric states. [20, 21] Oxidases are major generators of cell ROS, [22] and recent literature suggests that melanocytes and keratinocytes have high levels of NOX oxidases such as NADPH oxidase 1. [23] The NADPH oxidase 1 holoenzyme is a major producer of UV-induced ROS. [20] The oxidase is involved in activation of the PI3K/Akt signal pathway. [24] Apocynin may inhibit activity of other oxidases as well. Despite this poorly understood and likely complex mechanism, its biological effects in ROS reduction are exceptional. [25] Thus, despite the complex biological profile of apocynin it presented the best possible chance for functioning *in vivo*.

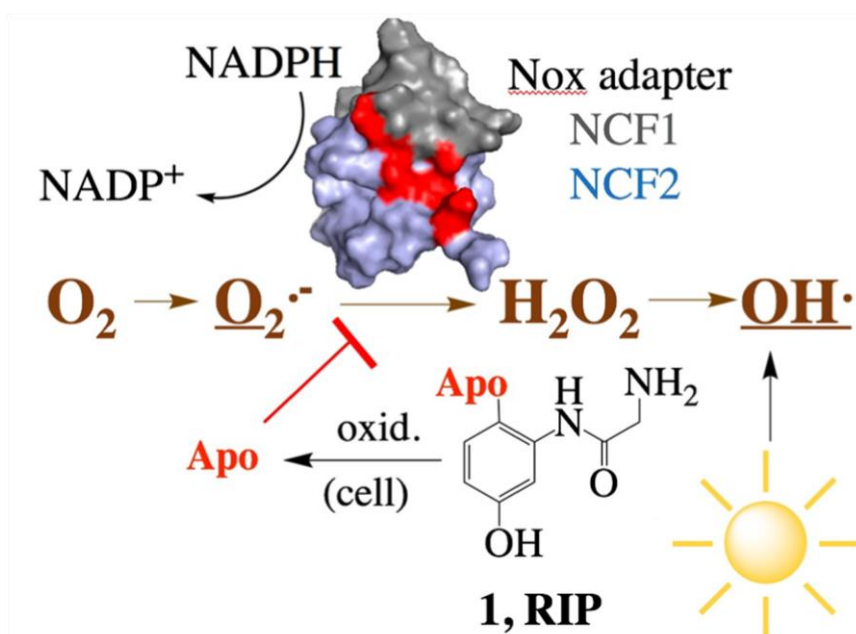


Figure 1: ROS (brown) are normally present but UV radiation enhances formation of highly toxic species (underlined) that damage DNA. RIP reagents, such as the apocynin-linked compound **1** shown, eject an oxidase inhibitor in high oxidative stress environments. Apocynin (red) binds NADPH oxidase-associated factors NCF1 and NCF2 to limit further ROS production. Structure from PDB 1K4U in reference 21.

2. Material and methods

2.1. Synthesis and characterization

Chemicals: Boc-sarcosine, trifluoroacetic acid (TFA) and dimethylformamide, chloromethyl methyl ether were purchased from Sigma-Aldrich Chemical Co. (St. Louis, MO, USA). Apocynin, 4-floro-3nitro phenol, pladium on carbon, 4'-Hydroxyacetophenone, 1-Fluoro-2-nitrobenzene, Triethylsilane, HATU were purchased from Fisher scientific international, Inc. All solutions were prepared with water purified by a Milli-Q system (Millipore, Bedford, MA, USA). All reagents used for buffer preparation were of analytical grade.

Full synthetic details and NMR and MS characterization data are provided in Supplementary material.

2.2. Oxidation study

2.2.1 Materials:

All stock solutions (0.1mM) of compound were dissolved in 25mM phosphate with various pH corresponding to the different working concentrations.

HPLC condition for oxidation studies: A Beckman Coulter's HPLC system consisting of a dual pump Model 126 with 32 Karat Software, a System Gold 168 detector and a System Gold 508 Auto Sampler was used. A reverse phase C-18 column (Synergi™ 4μm Hydro-RP 80Å, LC Column 100×4.6mm, Ea.) was used. The mobile phase consisted of HPLC grade Acetonitrile (Fisher Scientific), LCMS grade formic acid (Fisher scientific) and distilled water filtered through a Millipore Milli-Q water purification system. Solvent A for the mobile phase was 95% water, 5% Acetonitrile for oxidation study of **1** and 95% water, 5% Acetonitrile for oxidation studies of 1a-c. Solvent B is 95% acetonitrile and 5% water. The gradient was 0% B for 4 minute and 95% B over 16 minutes. Flow was 1ml/min. A detection wavelength of 250nm and 285nm was used for oxidation of **1**.

2.2.2 Methods:

HRP oxidation: A working solution (1mg **1** was dissolved in 30mL 0.08 mM hydrogen peroxide in 25 mM phosphate buffer, pH=7.0) was made. A 1mL sample was used as the no enzyme control. The reaction was 1mL of working solution and 0.1U HRP. After 60 mins, 1mL ethyl acetate was added, shaken, and extraction performed. The organic layer was analyzed by HPLC to quantify the relative amounts of **1** and apocynin. Moles were calculated using a standard of each compound and yields were calculated using integration. All determinations were carried out in triplicate on different days. On each occasion and new standards and samples were made.

Fenton reagent oxidation: The above working solution was mixed with 10μL Fe-solution (10 mM Fe(NH₄)₂(SO₄)₂•6 H₂O, 10 mM EDTA, pH 8) by centrifugation of Fe-solution placed on the cap of an Eppendorf tube. After 60mins of reaction, the reaction was processed as before.

KO₂ oxidation: 1mg **1** was dissolved in 30mL 25 mM phosphate buffer, pH=7. Solid KO₂ was premeasured into an 15mL falcon to give a final concentration of KO₂. After 60mins analysis proceeded as before.

UV Sensitivity of **1**: 1mg **1** was dissolved in 30mL 25 mM phosphate buffer, pH=7. 1mL was irradiated for 10 SED (10 min) using an Oriel Sol-UV-6 Solar Simulator, Oriel Instruments. After irradiation, analysis proceeded as before.

Oxidation studies of compound **2** were performed following the same procedure as **1**.

2.3. Antioxidant studies

2.3.1 pUC19 ASSAY

Reaction mixture were prepared with 1 µg/ µL pUC19, and 0.5 mM 2'-deoxyguanosine in 20mM pH 7.4 phosphate buffer. Reactions with **1** had a final concentration of 50 µM. Fenton conditions were as described above. After 20 minutes reactions were stopped by addition of 10 µl quench solution (0.5 M EDTA and 0.75M 2-mercaptoethanol in 6X agarose gel loading buffer). A 1% agarose gel was prepared containing 0.75 µg/mL ethidium bromide. From each reaction, 12 µL of quenched reaction was loaded per well. Gel electrophoresis was performed at 120 mV for 45 mins. Agarose gel images were analyzed by ImageQuant 6.0 software to determine the intensity of each band. Percentage of non-damaged DNA was calculated in each sample, by comparing the band intensity corresponding to super-coiled pUC19 in each sample, with DNA only control.

2.3.2 ABTS Assay

ABTS was dissolved in water to a 7 mM concentration. ABTS radical cation (ABTS•+) was produced by reacting ABTS stock solution with 2.45 mM potassium persulfate (final concentration) and allowing the mixture to stand in the dark at room temperature for 24 h before use. For the study, the ABTS•+ working solution was diluted with PBS, pH 7.4, to an absorbance of 0.70 (±0.05) at 734 nm. Then 100µL working solution was mixed with 100 µL of various concentrations of each solution in a 96 well microplate. After 6 minutes of incubation the plate was

read at 743nm for absorbance. Appropriate solvent blanks were also run in each assay. All determinations were carried out at least three times including the standards and controls. The percentage inhibition of absorbance at 734 nm is calculated by: $(Ac-At)/Ac \times 100\%$. The EC50 based on the Concentration-response curve for the absorbance at 734 nm for ABTS•+ as a function of concentration of antioxidant solution.

2.4. Drug releasing study in cells

2.4.1 Cell Culture

In these studies neonatal human keratinocytes were plated at a density of 0.60×10^6 cells/100 mm dish in EpiLife® supplemented medium (Gibco) and grown to a density of 80% confluence. The following experimental groups: 1) Control; 2) ssUVR; 3) 50 μ M **1**; and 4) ssUVR+50 μ M **1** were used unless otherwise noted.

2.4.2 Efficacy of RIP Reagent in Cellular Environment

Cells were allowed to attach for 24 h and incubated with **1** for 18 h before irradiation with 8 SED using a Oriel Sol-UV-6 Solar Simulator set to maximum power. Immediately after irradiation, fresh medium was replaced and cells were kept in 5% CO₂ humidified incubator at 37°C for 1.5 hr. After 1.5hr, cells were washed in cold PBS and detached from the dish with cell scraper in 1ml of cold PBS. Ethyl acetate was added 1:1 (v/v) to the cell suspension. Organic layer was then extracted and dried. Samples were resuspended in 100 μ L of acetonitrile and analyzed by direct injection into the HPLC as described above. All determinations were carried out at least three times.

2.4.3 Quantifying Damage by LC-MS

Fibroblast cells (8×10^6 per sample) in PBS were treated with **1** or PBS for 18 h at 37 °C. Then, sample cells were irradiated at 10 SED using an Oriel Sol-UV-6 Solar Simulator operating at 24 °C. All treatments were performed in quadruplicate. To isolate genomic DNA cells were trypsinized, washed, and lysed by freeze/thaw for four cycles. Then, DNA was isolated using a

Wizard Genomic DNA Purification Kit (Promega Corp) per kit instructions. DNA yield for each sample was quantified by A_{260} in triplicate. Digestion of DNA occurred using, the following procedure. DNA was denatured, placed on ice, and incubated with 0.2 U of bovine pancreas DNase I (Millipore Sigma) in 0.03 M ammonium acetate (pH 5.) at 45 °C for 2 h. The enzyme was then precipitated and spun down using ammonium bicarbonate (pH 8.0). Next, 5 mU of phosphodiesterase I (Worthington Biochemical Corp.) and 0.2 U of calf intestinal alkaline phosphatase (Thermo Fisher) were incubated at 37 °C for 2 h. Finally, enzymes were again precipitated. and samples resuspended in 200 μ L of LC-MS mobile phase.

LC-MS analysis was performed with a SCIEX 4000 QTRAP triple quad mass spectrometer with a turbo spray ion source interfaced with an Agilent 1260 HPLC. Injection volume was 5 μ L onto an Agela Technologies Optimix C18/amide column (2.1 x 50 mm, 5 μ m) flowing at 0.2 mL/min in HILIC mode at 20 °C. Solvent A was 95:5 water:acetonitrile and Solvent B was 95:5 acetonitrile:water, both with 0.1% formic acid. The following gradient was used: 0 min, 100% B; 2.5 min, 100% B; 7.6 min, 70% B; 9.4 min, 70% B; 10.4 min, 100% B. Selected ion monitoring in positive ion mode was used to detect 8-oxo-7,8-dihydro-2'-deoxyguanosine ($[M+H]^+$; $m/z = 284.1$). Peak areas were normalized per μ g of DNA.

2.4.4 DCFDA assay by flow cytometry

Cells were grown in 25 cm^2 tissue culture plates to 50% confluence. Then each plate was incubated with the listed compound for 18 hours. Cells were trypsinized, added, incubated for 30 min, and cells washed with HBSS twice. Each sample was irradiated and then 5 μ M DCF-DA (Sigma Aldrich) was added. Incubation for 30 min, washing, and DCF fluorescence was obtained in using BD FACS Canto flow cytometer by exciting at 485 nm and emission at 535nm after eliminating 7AAD positive cells. Percentage of cells with high DCF fluorescence were compared among different treatments. Data shown are the average of three biological replicates.

3. Result and discussion

We envisioned that the ROS-initiated release of apocynin would occur as shown in Figure 2 and a more detailed mechanism is shown in SI Scheme 1. Because the phenol of apocynin is essential to its unique biochemical mechanism, covalent attachment to the ROS-sensitive motif through an would block apocynin activity except under oxidative stress conditions. To examine the reaction, two derivatives were synthesized: the RIP reagent (**1**, structure shown) and a control molecule (**2**) where the phenol is not present to prevent oxidation and subsequent cyclization. Compound **1** was made in five steps with a net 25% yield and **2** was made in four steps in 45% yield (see SI for NMRs and synthetic details)

The oxidation reaction of **1** was examined (Figure 2A) under Fenton conditions, which generate hydroxyl radical. The Fenton conditions were 0.1 mM $\text{Fe}(\text{NH}_4)_2(\text{SO}_4)_2 \cdot 6\text{H}_2\text{O}$, and 0.08 mM H_2O_2 in pH 7.0 phosphate buffer and the concentration of **1** was 0.1 mM. Extraction was performed since apocynin is not soluble in buffered solutions. After extraction with ethyl acetate the aqueous and organic layers were analyzed by HPLC. Under our conditions, **1** eluted near 10 min, whereas apocynin eluted near 12 min (Figure 2B). The second reaction product, **1^{ox}**, is observed in the aqueous layer and has a characteristic absorbance at 375 nm as does a variant of **1^{ox}** identified in a previous manuscript. [17] Exposure to Fenton conditions in phosphate buffer led to formation of products **1^{ox}** and apocynin, whereas in the absence of Fenton reagent no reaction was observed (Figure 2B). Quantitative analysis of the organic layer indicated that under these Fenton conditions, 85% (+/- 2%) of **1** was converted to products (Figure 2C). This is close to the expected yield based on the concentrations of **1** and H_2O_2 , indicating that the first oxidative equivalent of Fenton reagent reacts with **1** completely. Both products were collected, and MS analysis confirmed expected product identities (Figure 2C).

We next examined the reaction of **1** with various ROS forms encountered under cellular conditions Figure 2D. After 1 hr in Fenton conditions, 15% (+/- 2%) **1** remained. In experiments lacking $\text{Fe}(\text{NH}_4)_2(\text{SO}_4)_2$ and only containing hydrogen peroxide we find an insignificant loss of **1** after 1 hr. Importantly, the reaction is diffusional and first order in both Fenton reagents (SI Figure 1). This indicates that self-cyclization of **1** will be strongly correlated to the total amount present in cells. After a 1 hr exposure to 0.08 mM KO_2 63% (+/-8%) of **1** remained. Oxidase activation was examined using 0.01 mU of HRP enzyme and 0.08 mM H_2O_2 . Under these conditions 30% (+/- 5%) remained after 1 h. We examined the control compound **2**, which lacks a phenol important to

oxidation, under the same conditions. Compound **2** was resistant to oxidation (Figure 2D, purple) under the same conditions, in all cases.

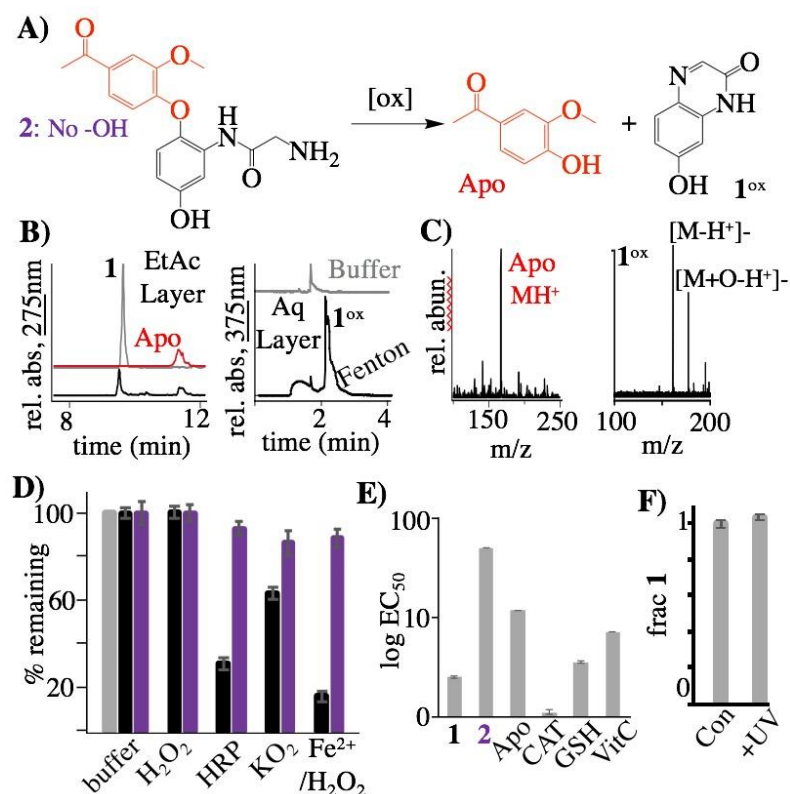


Figure 2: (A) Proposed reaction of **1** to release apocynin and generate **1^{ox}**. The control compound **2** lacks an oxidizable phenol. (B) HPLC analysis of **1** incubated in phosphate buffer (gray trace) and under Fenton conditions (black trace); the organic (left) and aqueous (right) layers were analyzed. Pure Apo was also analyzed (red trace), and peak corresponding to **1^{ox}** and Fenton reagents are indicated. (C) MS of isolated products. (D) Sensitivities of **1** (black) and **2** (purple) to various ROS forms. (E) Antioxidant capacity as measured by ABTS assay. The obtained EC₅₀ values are shown. (F) Fraction of **1** in solution not subjected to irradiation and irradiated with 10 SED.

We then assessed antioxidant activity of the RIP reagent **1** (Figure 2E for EC₅₀). To determine antioxidant capacity a 2,2'-azino-bis(3-ethylbenzothiazoline-6-sulphonic acid) (ABTS) assay was performed. In the assay, green ABTS (7 mM) radicals are induced from persulfate (2 mM), and the ability of antioxidants to reduce color formation is evaluated over a concentration range to obtain an EC₅₀ value (SI Figure 2 for data). In the presence of 10 μM **1**, rapid inhibition was observed, whereas **2** at the same concentration had limited activity. Compound **1** had an EC₅₀ value of 2.4 (+/-0.1) μM, whereas the EC₅₀ of **2** is 60 (+/- 1) μM. Apocynin, catalase, glutathione, and vitamin C had EC₅₀ values of 11.7 (+/- 0.4), 0.7 (+/- 0.1), 3.5 (+/- 0.2), and 7 (+/- 0.1) μM, respectively. Thus, **1** has modest antioxidant ability relative to common antioxidants but these reactions are

required to release the bioactive molecule.

It is important that **1** be stable to UVR exposure (Figure 2F). To test this, **1** (100 μM) in phosphate buffer (pH 7) was irradiated for a total of 10 Standard Erythematous Dose (SED) units. Under these conditions, **1** is not degraded. In summary, these data show that **1** is oxidized by various ROS, has antioxidant capacity similar to those of common antioxidants and that the oxidation liberates apocynin, a bioactive oxidase inhibitor.

Next, we analyzed the ability of **1** to prevent DNA damage in an *in vitro* DNA nicking assay (Figure 3A). The concentration of pUC19 plasmid was 1000 ng/ μL . After 1 hr incubation under Fenton conditions, 31% (+/-3%) of the plasmids were nicked. No nicking was observed under Fenton conditions in the presence of 50 μM **1** or **1** without Fenton reagent.

We then evaluated the cytotoxicity of **1** to primary keratinocytes in culture. After three days of incubation with **1** no cytotoxicity was observed except at the highest dose tested. At the high dose of 100 μM , a 15% (+/- 3%) reduction in viability was observed (Figure 3B). We also examined the effect of **2**, which is not oxidizable, and a compound that is oxidizable but does not eject apocynin (SI Figure 3). The five step synthesis is listed in SI section 4.3. As expected **2** showed limited cytotoxicity while the non-oxidizable derivative of **1** showed more cytotoxicity than **1**. To evaluate what was occurring inside primary keratinocytes were treated with 50 μM **1** or not and irradiated. The organic layer was extracted and quantified (SI Figure 4 for chromatograms). In cells treated with **1** but not subjected to UVR, little apocynin was detected (0.03 +/- 0.02 pmol). In cells that were treated with **1** and irradiated 0.97 (+/- 0.07) pmol of apocynin were detected (Figure 3C), thereby confirming that self-cyclization and apocynin release occurs within a cellular environment. Based on this analysis, the concentration of apocynin within the cells is approximately 28 μM , this is a level that is known to cause inhibitory effects. We also observed **1** inside of cells at a concentration of 190 μM . Thus, little apocynin is released without UVR treatment and UVR leads to ~17% release of apocynin.

Irradiation of primary keratinocytes with 10 SED reduced viability to 63% (+/-5%) relative to DMSO-treated control cultures (Figure 3D). Cells were also treated with 50 μM **1**, 50 μM apocynin, 50 μM glutathione, or 3 U catalase without irradiation. Both apocynin and catalase

slightly but significantly enhanced growth to 106% (+/-2%) and 110% (+/- 3%) relative to DMSO-treated controls ($p < 0.05$). Neither **1** nor glutathione influenced viability at this concentration (Figure 3D). Higher concentrations of apocynin, glutathione, and catalase were cytotoxic (data not shown). After the 10 SED irradiation, compound **1** increased viability to 88% (+/-5%) relative to the control, while irradiated cells pretreated with apocynin showed a more modest rescue to 75% (+/-2%) (Figure 3D). **1** is two times better at entering a cell than apocynin (SI Figure 5), but does not affect viability without activation. Next we examined if **2**, which cannot be oxidized, rescued cells from UVR stress. SI Figure 3 shows little rescue in the presence of UVR. Similarly we examined a compound that is oxidizable but lacks apocynin release (SI Figure 3). Limited rescue in the presence of UVR stress is observed.

We validated if apocynin was inhibiting NOX enzymes or is just an antioxidant (SI Figure 6). Cells were treated with apocynin and the phosphorylation status of AKT, a downstream protein dependent on NOX1 activity, quantified²⁴. An in-cell western for phosphorylation of AKT at Ser473, which is phosphorylated downstream of NOX activity, was performed. Apocynin reduced the amount of phosphorylated serine by 21 (+/-9)% in the presence of UVR. The p-value was less than 0.02. To further confirm the ability of **1** to reduce oxidative stress in cells we examined the amount of 8-oxo-7,8-dihydro-2'-deoxyguanosine relative to non-UVR treated cells via LC-MS (Figure 3E). Because of the large quantity of cells needed primary fibroblasts were used. In this assay the integrated intensities at 284 m/z were compared to the total amount of DNA recovered. For simplicity total integrated values are reported per million. We found that UVR treatment raised the relative level of the lesion to 2.03 (+/- 0.19) from 1.41 (+/- 0.05) Int/ μ g DNA with a p-value less than 0.01. Treatment of **1** prior to UVR lead to a reduction of the lesion back to 1.39 (+/- 0.21), which is not statistically different compared to untreated cells. Finally, **1** alone does not change the amount of lesion found. Subsequent confirmatory experiments utilized the common DCF-DA oxidative stress assay (Figure 3F). Though DCF-DA has known issues, mainly dealing with the amount of incubation time leading to indiscriminate activation of the dye[26], the same trend in the data is observed. Thus, of the compounds tested, **1** had the smallest effect on cell growth in non-irradiated cells and the ability to protect cells from UVR.

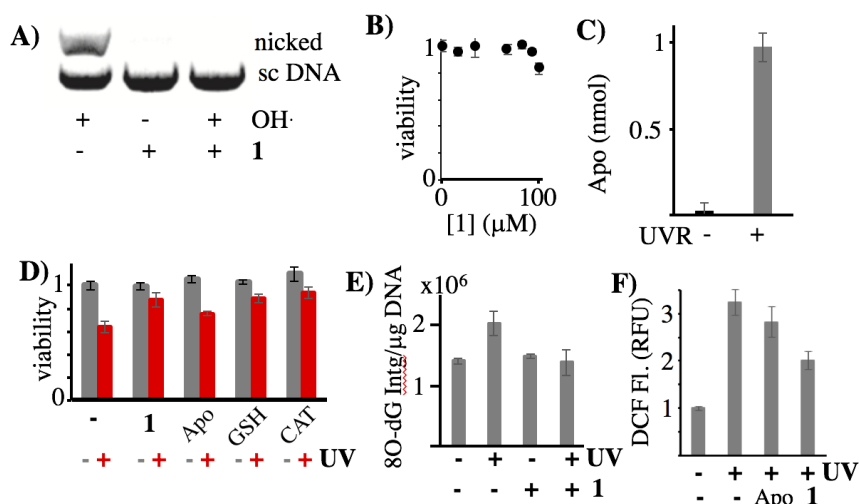


Figure 3: (A) Gel electrophoretic separation of supercoiled and nicked plasmid in the presence and absence of Fenton reagent and compound **1**. (B) Viability of primary keratinocytes in a range of concentrations of **1**. (C) Production of Apo in skin cells treated with 50 μM **1** with and without irradiation with 10 SED. (D) Viability of primary keratinocytes without (gray bars) and with 10 SED UVR (red bars) in the presence of the indicated antioxidants. (E) Relative LCMS quantification of 8-oxo-7,8-dihydro-2'-deoxyguanosine under UVR and **1** treatment. (F) Dichlorodihydrofluorescein diacetate fluorescence measurements under UVR and **1** treatment.

We then used a human skin explant model to evaluate the effect of topical treatment with **1** on UV-induced damage (Figure 4A). In this model, topical treatments, mimicking use of sunscreen, can be tested without compromising the dermis. Discarded and deidentified human skin was obtained from donors undergoing elective surgical procedures. Human skin was used as rodent models do not recapitulate human biochemistry due to the amount of hair. Subcutaneous fat tissue was removed from the skin, and skin was cut into 3.5 cm diameter circles and placed into culture dishes with DMEM/F12 media without phenol red, supplemented with growth factors. The dermal side was in contact with the medium, and the epidermal was exposed to air. A solution of 50 μM **1** or DMSO control solution was spread on the skin and allowed to dry overnight. Note that skin is much more resistant to UVR than naked cells so a 25 SED UVR exposure was used. After exposure skin was homogenized, protein was extracted, and DNA damage signaling quantified by western blotting. UVR induced strong expression of the DNA repair signaling protein p53 at 24 h post irradiation. Treatment of **1** without UVR caused no increase in expression of p53. Importantly, p53 expression was reduced by 46% (+/-5%) in skin treated topically with **1** and then irradiated (Figure 4B).

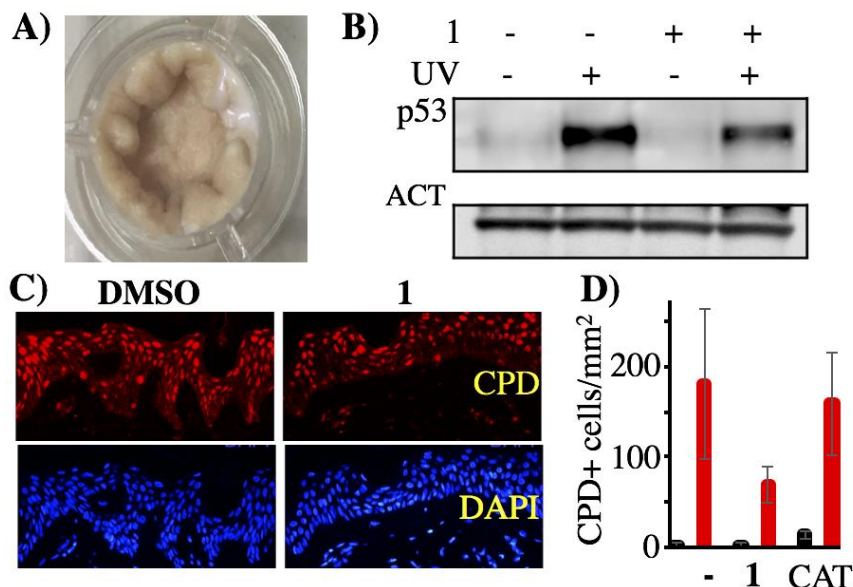


Figure 4: (A) Representative image of skin explant. (B) Western blot analysis of p53 production in skin explants treated or not with **1** and subjected or not to UVR. Actin protein shown as a control. (C) Representative immunofluorescence images of skin explants treated with DMSO or **1** and subjected to 10 SED irradiation. Red indicates the presence of CPDs; nuclei were stained with DAPI (blue). (D) Quantification of CPD-positive cells per mm² of non-irradiated (black bars) and irradiated (red bars) skin treated with DMSO (-), compound **1**, or catalase (CAT).

We then directly evaluated DNA damage in skin explants by staining for cyclobutane dimers (CPDs). Skin explants were treated with RIP reagent **1** (50 μM) or catalase (3U) and dried overnight. At 24 h after 25 SED irradiation, explants were subjected to immunofluorescence imaging (Figure 4C). Experiments were performed on three separate skin explants per condition and quantification was performed using ImageJ software at 20 different locations per skin explant (Figure 4D). Cells (identified by staining with DAPI) that co-localized with CPD signal (3 fold above background) were scored as damaged. Without irradiation, few cells were positive for CPD (2 +/-2 cells/mm²). Upon UVR exposure, 180 (+/- 82) CPD-positive cells per mm² were detected in DMSO-treated control explants. Treatment with **1** without UVR did not have a significant effect (2 +/-2 CPD⁺ cells/mm²) but catalase treatment did (13 +/- 4 CPD⁺ cells/mm²), indicating some resting reductive stress. After UVR exposure, catalase-treated samples had 160 (+/-60) CPD-positive cells per mm², not significantly different from the control UVR-treated explants. In contrast, treatment with **1** significantly reduced the number of CPD-positive cells per mm² to 70 (+/- 20) relative to the control explants (p<0.0005). Thus, the RIP reagent **1** greatly reduced DNA damage and damage signaling when applied topically to human skin explants.

In conclusion, we have developed an ROS-controlled antioxidant, RIP reagent **1**, that after oxidative reaction (antioxidant function) releases a NOX inhibitor known as apocynin. The ROS-activation is dependent on a key phenol in the molecule that leads to self-cyclization and release of the NOX inhibitor. The molecular design of the ROS-initiated protective reagent is an alternative to the well-known boron ester and quinone methide chemistries. Reagent **1** did not alter viability of cultured skin cells and prevented UVR-induced cell death to a similar extent as other tested antioxidants. In a human skin explant model, **1** applied topically reduced the formation of cyclobutane dimers and DNA repair signaling. Thus, the described RIP reagent is a catalytic antioxidant activated by high oxidative stress environments like UVR irradiation and these reagents have potential for uses in sunscreens.

Acknowledgements

We acknowledge the R. Marshall Wilson Mass Spectrometric Facility of the Department of Chemistry, University of Cincinnati. This study was supported by Department of Defense grant W81XWH-16-1-0489 to EJM and ALK.

References

- [1] A.P. Schuch, N.C. Moreno, N.J. Schuch, C.F.M. Menck, C.C.M. Garcia, Sunlight damage to cellular DNA: Focus on oxidatively generated lesions, *Free Radic Biol Med* 107 (2017) 110-124.
- [2] N.P. Smit, F.A. Van Nieuwpoort, L. Marrot, C. Out, B. Poorthuis, H. Van Pelt, J.R. Meunier, S. Pavel, Increased melanogenesis is a risk factor for oxidative DNA damage—study on cultured melanocytes and atypical nevus cells, *Photochemistry and photobiology* 84(3) (2008) 550-555.
- [3] L. Denat, A.L. Kadarko, L. Marrot, S.A. Leachman, Z.A. Abdel-Malek, Melanocytes as instigators and victims of oxidative stress, *The Journal of investigative dermatology* 134(6) (2014) 1512-1518.
- [4] S. Premi, S. Wallisch, C.M. Mano, A.B. Weiner, A. Bacchiocchi, K. Wakamatsu, E.J. Bechara, R. Halaban, T. Douki, D.E. Brash, Chemiexcitation of melanin derivatives induces DNA photoproducts long after UV exposure, *Science (New York, N.Y.)* 347(6224) (2015) 842-847.
- [5] L. Zheng, M.M. Greenberg, Traceless Tandem Lesion Formation in DNA from a Nitrogen-Centered Purine Radical, *J Am Chem Soc* 140 (2018) 6400-07.
- [6] G. Li, T. Bell, E.J. Merino, Oxidatively activated DNA-modifying agents for selective cytotoxicity, *ChemMedChem* 6(5) (2011) 869-75.
- [7] Y. Kuang, K. Balakrishnan, V. Gandhi, X. Peng, Hydrogen peroxide inducible DNA cross-linking agents: targeted anticancer prodrugs, *J Am Chem Soc* 133(48) (2011) 19278-81.
- [8] D. Lee, S. Park, S. Bae, D. Jeong, M. Park, C. Kang, W. Yoo, M.A. Samad, Q. Ke, G. Khang, Hydrogen peroxide-activatable antioxidant prodrug as a targeted therapeutic agent for ischemia-reperfusion injury, *Scientific*

reports 5 (2015) 16592.

- [9] T.T. Hoang, T.P. Smith, R.T. Raines, A Boronic Acid Conjugate of Angiogenin that Shows ROS- Responsive Neuroprotective Activity, *Angewandte Chemie* 129(10) (2017) 2663-2666.
- [10] S. Mori, K. Morihira, T. Okuda, Y. Kasahara, S. Obika, Hydrogen peroxide-triggered gene silencing in mammalian cells through boronated antisense oligonucleotides, *Chemical science* 9(5) (2018) 1112-1118.
- [11] D. Chen, G. Zhang, R. Li, M. Guan, X. Wang, T. Zou, Y. Zhang, C.-R. Wang, C. Shu, H. Hong, Biodegradable, Hydrogen Peroxide and Glutathione Dual Responsive Nanoparticles for Potential Programmable Paclitaxel Release, *J Am Chem Soc* 140 (2018) 7373-76.
- [12] S. Daum, S. Babiy, H. Konovalova, W. Hofer, A. Shtemenko, N. Shtemenko, C. Janko, C. Alexiou, A. Mokhir, Tuning the structure of aminoferrocene-based anticancer prodrugs to prevent their aggregation in aqueous solution, *Journal of inorganic biochemistry* 178 (2018) 9-17.
- [13] C. Yik-Sham Chung, G.A. Timblin, K. Saijo, C.J. Chang, Versatile Histochemical Approach to Detection of Hydrogen Peroxide in Cells and Tissues Based on Puromycin Staining, *Journal of the American Chemical Society* 140(19) (2018) 6109-6121.
- [14] H.J. Forman, A. Bernardo, K.J. Davies, What is the concentration of hydrogen peroxide in blood and plasma?, *Archives of biochemistry and biophysics* 603 (2016) 48-53.
- [15] F.S. Thowfeik, S.F. AbdulSalam, M. Wunderlich, M. Wyder, K.D. Greis, A.L. Kadekaro, J.C. Mulloy, E.J. Merino, A ROS- Activatable Agent Elicits Homologous Recombination DNA Repair and Synergizes with Pathway Compounds, *Chembiochem : a European journal of chemical biology* 16(17) (2015) 2513-2521.
- [16] A.K. Vadukoot, S.F. AbdulSalam, M. Wunderlich, E.D. Pullen, J. Landero-Figueroa, J.C. Mulloy, E.J. Merino, Design of a hydrogen peroxide-activatable agent that specifically targets cancer cells, *Bioorganic & medicinal chemistry* 22(24) (2014) 6885-92.
- [17] S.F. AbdulSalam, P.N. Gurjar, H. Zhu, J. Liu, E.S. Johnson, A.L. Kadekaro, J. Landero-Figueroa, E.J. Merino, Self-Cyclizing Antioxidants to Prevent DNA Damage Caused by Hydroxyl Radical, *Chembiochem : a European journal of chemical biology* 18(20) (2017) 2007-2011.
- [18] S.F. AbdulSalam, F.S. Thowfeik, E.J. Merino, Excessive Reactive Oxygen Species and Exotic DNA Lesions as an Exploitable Liability, *Biochemistry* 55(38) (2016) 5341-52.
- [19] X. Ao, S. Bright, N. Taylor, R. Elmes, 2-Nitroimidazole based fluorescent probes for nitroreductase; monitoring reductive stress in cellulose, *Organic & biomolecular chemistry* 15(29) (2017) 6104-6108.
- [20] L.H. Tanriverdi, H. Parlakpinar, O. Ozhan, N. Ermis, A. Polat, N. Vardi, K. Tanbek, A. Yildiz, A. Acet, Inhibition of NADPH oxidase by apocynin promotes myocardial antioxidant response and prevents isoproterenol-induced myocardial oxidative stress in rats, *Free radical research* 51(9-10) (2017) 772-786.
- [21] P. Jantaree, K. Lirdprapamongkol, W. Kaewsri, C. Thongsornkleeb, K. Choowongkamon, K. Atjanasuppat, S. Ruchirawat, J. Svasti, Homodimers of vanillin and apocynin decrease the metastatic potential of human cancer cells by inhibiting the FAK/PI3K/Akt signaling pathway, *Journal of agricultural and food chemistry* 65(11) (2017) 2299-2306.
- [22] H.J. Forman, Redox signaling: An evolution from free radicals to aging, *Free Radic Biol Med* 97 (2016) 398-407.
- [23] A. Valencia, I.E. Kochevar, Nox1-based NADPH oxidase is the major source of UVA-induced reactive oxygen species in human keratinocytes, *Journal of Investigative Dermatology* 128(1) (2008) 214-222.
- [24] K. Ito, A. Ota, T. Ono, T. Nakaoka, M. Wahiduzzaman, S. Karnan, H. Konishi, A. Furuhashi, T. Hayashi, Y. Yamada, Inhibition of Nox1 induces apoptosis by attenuating the AKT signaling pathway in oral squamous cell carcinoma cell lines, *Oncology reports* 36(5) (2016) 2991-2998.
- [25] M.M. Castro, E. Rizzi, G.J. Rodrigues, C.S. Ceron, L.M. Bendhack, R.F. Gerlach, J.E. Tanus-Santos, Antioxidant treatment reduces matrix metalloproteinase-2-induced vascular changes in renovascular hypertension, *Free Radic Biol Med* 46(9) (2009) 1298-1307.
- [26] B. Kalyanaraman, V. Darley-Usmar, K.J. Davies, P.A. Dennery, H.J. Forman, M.B. Grisham, G.E. Mann, K. Moore, L.J. Roberts II, H. Ischiropoulos, Measuring reactive oxygen and nitrogen species with fluorescent probes: challenges and limitations, *Free Radic Biol Med* 52(1) (2012) 1-6.

Highlights

- New antioxidants are needed to prevent melanoma by reducing skin radicals and ROS
- A ROS-induced protection reagent quenches ROS leading to release of apocynin
- In cells apocynin was released only with UV and reduced DNA lesions
- Topical treatment of human skin explants reduced pyrimidine dimers and p53

Accepted manuscript